Published in final edited form as:
Science. 2013 July 26; 341(6144): 406–410. doi:10.1126/science.1235103.

Reprogramming of Intestinal Glucose Metabolism and Glycemic Control in Rats After Gastric Bypass

Nima Saeidi[1,2,3], **Luca Meoli**[1], **Eirini Nestoridi**[1], **Nitin K. Gupta**[1], **Stephanie Kvas**[1], **John Kucharczyk**[1], **Ali A. Bonab**[2], **Alan J. Fischman**[2], **Martin L. Yarmush**[2,3], and **Nicholas Stylopoulos**[1]

[1]Center for Basic and Translational Obesity Research, Division of Endocrinology, Boston Children's Hospital, Harvard Medical School, Boston, MA 02115, USA

[2]Shriners Hospital for Children, Boston, MA 02114, USA

[3]Center for Engineering in Medicine, Massachusetts General Hospital, Harvard Medical School, Boston, MA 02114, USA

Abstract

The resolution of type 2 diabetes after Roux-en-Y gastric bypass (RYGB) attests to the important role of the gastrointestinal tract in glucose homeostasis. Previous studies in RYGB-treated rats have shown that the Roux limb displays hyperplasia and hypertrophy. Here, we report that the Roux limb of RYGB-treated rats exhibits reprogramming of intestinal glucose metabolism to meet its increased bioenergetic demands; glucose transporter-1 is up-regulated, basolateral glucose uptake is enhanced, aerobic glycolysis is augmented, and glucose is directed toward metabolic pathways that support tissue growth. We show that reprogramming of intestinal glucose metabolism is triggered by the exposure of the Roux limb to undigested nutrients. We demonstrate by positron emission tomography–computed tomography scanning and biodistribution analysis using 2-deoxy-2-[18F]fluoro-D-glucose that reprogramming of intestinal glucose metabolism renders the intestine a major tissue for glucose disposal, contributing to the improvement in glycemic control after RYGB.

Roux-en-Y gastric bypass (RYGB) induces substantial and sustained weight loss and is a highly effective treatment for severe obesity (1-3). The results of three recent prospective studies suggest that RYGB is the best treatment option for obesity-related diabetes (4-6). Interestingly, the improvement in glucose homeostasis occurs early after the RYGB procedure, before any appreciable weight loss, and patients are often able to discontinue their antidiabeticmedications before hospital discharge (4, 5, 7, 8). The precise mechanisms underlying the resolution of diabetes after RYGB have not been determined (3, 8-10). Several studies in rodents and one study in humans have previously described that the Roux limb displays morphological changes, characterized by hypertrophy and hyperplasia after RYGB (11-16). However, the importance of the morphological adaptation of the Roux limb,

Corresponding author: Nicholas Stylopoulos, MD, Assistant Professor of Pediatrics, Center for Life Science, Children's Hospital Boston, Endocrinology, Room 16066, 3 Blackfan Circle, Boston MA 02115, Phone: 617-919-2714, Nicholas.Stylopoulos@childrens.harvard.edu.

in itself, in themetabolic effects of RYGB remains largely unknown. Because the construction of the Roux limb is one of the fundamental components of the RYGB procedure (Fig. 1A) (17, 18), we hypothesized that the beneficial effect of RYGB on glucose homeostasis may stem from changes in the metabolism within this reconfigured jejunal segment to meet the increased bioenergetic demands of tissue growth and maintenance, possibly in response to its exposure to undigested nutrients. To study the Roux limb, we performed RYGB in rats (19). RYGB led to substantial and sustained weight loss and improvement in glucose metabolism in diet-induced obese (DIO) rats, recapitulating the effects observed in humans (fig. S1, A to E). RYGB also improved glycemic control in two nonobese, diabetic rodent models with impaired insulin secretion: streptozotocin (STZ)–induced diabetic and Goto- Kakizaki (GK) rats (Fig. 1, B to D, and fig. S1, F to I). We also observed intestinal remodeling, characterized by increased intestinal mass due to hyperplasia and hypertrophy, in the Roux limb of RYGB-treated rats (figs. S2 to S4 and supplementary text 1). To test our hypothesis, we initially sought to identify possible metabolic changes in the Roux limb of RYGB-treated rats. We compared its metabolic profile with the profile of corresponding segments of the jejunum of sham-operated rats, using a quantitative polar metabolomic profiling platform. Themetabolomic profiling showed increased concentrations of glucose-6-phosphate, d-gluconate, 6-phospho-d-gluconate and nicotinamide adenine dinucleotide phosphate (NADP+) in the Roux limb, suggesting that the oxidative phase of the pentose phosphate pathway (PPP) is stimulated (fig. S5, A and B, and table S1). The changes in the metabolites of the nonoxidative phase of the PPP did not reach statistical significance, but there was an increase in the intermediates of the pyrimidine and purine biosynthetic pathways. Lactate was increased, whereas there was a decrease or no change in the intermediates of the tricarboxylic acid (TCA) cycle. The serine and the hexosamine biosynthetic pathways, two metabolic pathways that branch off from glycolysis, were also augmented. The glutamine/glutamate pathway was enriched, and the metabolism of several other amino acids appeared to be enhanced. This metabolic profile of the Roux limb indicates that glycolysis may be up-regulated in favor of accumulation of glycolytic intermediates that are shunted to metabolic pathways that support cellular growth and proliferation (fig. S5, A and B, and table S1). We next examined gene and protein expression patterns of enzymes involved in glucose metabolism. In comparison with corresponding segments of the jejunum of sham-operated rats, the Roux limb of RYGB-treated rats showed increased RNA and protein levels of hexokinase 2 (HK2), glyceraldehyde 3-phosphate dehydrogenase (GAPDH), and lactate dehydrogenase (LDH), which are key glycolytic enzymes (Fig. 2, A to C, and fig. S5C). M2 isoform expression of pyruvate kinase (PKM2) and phosphorylated PKM2 were also up-regulated in the Roux limb, further suggesting an increase in aerobic glycolysis to generate upstream glycolytic intermediates that are diverted into anabolic pathways (Fig. 2, A and B) (20, 21). The decreased glucose flux through the TCA cycle is also supported by the higher expression levels of pyruvate dehydrogenase kinase 1 (PDHK1), which phosphorylates and inactivates pyruvate dehydrogenase (PDH) (Fig. 2C). There was also an increase in the protein levels of both G and H forms and the enzymatic activity of glucose-6-phosphate dehydrogenase (G6PD), the rate-limiting enzyme of the PPP (Fig. 2, C and D). RNA levels of key enzymes of gluconeogenesis were suppressed or unchanged in the Roux limb of RYGB-treated rats (fig. S5D). We also detected augmented RNA and protein levels of factors and enzymes

involved in the biosynthesis of cholesterol in the Roux limb of RYGB-treated rats (Fig. 2, E to G, and fig. S6A). Cholesterol is essential for cellular growth and proliferation. The up-regulation of intestinal cholesterol biosynthesis may further explain the enhanced utilization of glucose by the Roux limb through the PPP, because the PPP provides a reduced form of NADP+ (NADPH), which is involved as a donor of reducing equivalents in cholesterol biosynthesis. The expression of low-density lipoprotein receptor (LDLR) was also higher in the Roux limb, suggesting that cholesterol uptake may also be augmented (Fig. 2, E to G, and fig. S6B). The hepatic cholesterol biosynthetic pathway was not changed (fig. S6C). Serum and hepatic lipid profiles were improved after RYGB (fig. S6, D to I). Taken together, our results support our hypothesis that the Roux limb of RYGB-treated rats exhibits reprogramming of intestinal glucose metabolism to meet the increased anabolic demands of intestinal tissue growth and maintenance. We also found that the PI3K/AKT/mTOR signaling pathway was activated in the Roux limb of RYGB-treated rats, which also indicates that there is augmented anabolic activity and increased glucose utilization (fig. S7) (21). To confirm that RYGB induces enhanced intestinal glucose uptake and utilization, we performed positron emission tomography–computed tomography (PET/CT) scanning using 2-deoxy-2-[18F]fluoro-D-glucose ([18F]FDG). These experiments were done with RYGB-treated and sham-operated DIO, STZinduced diabetic, and GK rats. [18F]FDG is taken up at a rate proportional to the rate of glucose utilization within a given tissue. There was intense [18F]FDG uptake by the Roux limb of all groups of RYGB-treated rats in comparison with the jejunum of sham-operated rats (Fig. 3A and movie S1). To further characterize the reprogramming of intestinal glucose metabolism in the Roux limb, we focused our study on basolateral glucose transporters, since in PET/CT scanning, [18F]FDG is administered intravenously and enters the intestinal cells through their basolateral and not their luminal side. The Roux limb of RYGB-treated rats displayed an increase in RNA and protein levels of glucose transporter-1 (GLUT-1) but no significant change in GLUT-2 and GLUT-3 levels (Fig. 3, B and C, and fig. S8, A to C). GLUT-1 is normally abundantly present in fetal intestine but progressively disappears until it is barely detected in adult intestine (22). It is considered to play a role in early intestinal tissue growth in the fetus (23). PET/CT scanning with or without the administration of phloretin, a GLUT-1 inhibitor, showed that phloretin substantially blunted [18F]FDG uptake by the Roux limb (Fig. 3D and fig. S8D). These results suggest that increased intestinal glucose uptake is primarily mediated through GLUT-1 after RYGB. To quantify the relative contribution of the intestine to whole-body glucose disposal, we performed biodistribution analysis using [18F]FDG in RYGB-treated and sham-operated rats. The intestine exhibited the highest rate of glucose uptake and became a major tissue for glucose disposal after RYGB (Fig. 3E). Specifically, glucose disposal per gram of tissue doubled in the intestine of RYGB-treated rats, with the glucose uptake by the Roux limb and common limb being higher in comparison with the glucose uptake by the jejunum of sham-operated rats (Fig. 3, E and F). We observed interanimal variability in the intestinal glucose uptake of RYGB-treated rats, and this variability correlated with the degree of intestinal remodeling (fig. S9A). Importantly, there was a positive correlation between the improvement in glycemic control after RYGB and the intestinal glucose uptake (fig. S9, B and C). Consistent with improved whole-body glucose disposal, the [18F]FDG blood signal was lower in RYGB-treated rats, because they displayed a higher rate of [18F]FDG disposal from the blood into the tissues in comparison

with sham-operated rats (Fig. 3G). These data demonstrate that reprogramming of intestinal glucose metabolism, marked by enhanced intestinal GLUT-1–mediated basolateral glucose uptake and utilization, contributes to the improvement in glycemic control after RYGB, independently of weight loss, improved insulin secretion, or improved insulin sensitivity (supplementary text 2). RYGB alters the flow of nutrients and reroutes undigested nutrients to the Roux limb (Fig. 1A). We wanted to investigate whether intestinal remodeling and reprogramming of intestinal glucose metabolism are triggered by the exposure of the Roux limb to undigested nutrients. To this end, we developed a rat model in which a loop of jejunum is transected and transposed between the esophagus and the stomach without performing any other anatomic alterations of the RYGB procedure [esophago-stomach jejunal loop interposition (ES-JLI) model] (Fig. 4A and movie S2). This transposed jejunal loop resembles the Roux limb of RYGB as it is exposed to undigested nutrients. ES-JLI–treated DIO and GK rats exhibited improved glycemic control, similar to RYGB-treated rats (fig. S10). We observed the same morphological adaptation between the transposed jejunal loop of ES-JLI– treated rats and the Roux limb of RYGB-treated rats. GLUT-1 and HK2 RNA and protein levels were increased in the transposed jejunal loop of ES-JLI treated rats, and [18F]FDG PET/CT scanning also showed intense [18F]FDG uptake by the transposed jejunal loop (Fig. 4, B and C). These data are consistent with our hypothesis that intestinal remodeling and reprogramming of intestinal glucose metabolism are triggered by the exposure of the Roux limb to undigested nutrients. To further support this hypothesis, we compared gene expression levels of key factors and enzymes involved in glucose and cholesterol metabolism between the various intestinal segments of RYGB-treated rats and corresponding segments of the intestine of sham-operated rats. A gradient in the change in RNA levels of key factors and enzymes involved in glucose uptake and utilization and in cholesterol biosynthesis and uptake was observed along the altered nutrient flow path in the intestine of RYGB-treated rats (figs. S11 and S12). The highest increase was detected in the Roux limb, which is exposed to undigested nutrients, but no change was found in the biliopancreatic limb, which is exposed to the gastric, hepatic, and pancreatic secretions but no nutrients, or in the distal common limb, which is exposed to fully digested nutrients. The effectiveness of RYGB in the resolution of type 2 diabetes attests to the important role of the gastrointestinal tract in glycemic control. Most studies have attributed the improved glucose metabolism to a number of advantageous changes in the levels of gastrointestinal hormones that control glucose homeostasis and occur after RYGB, with enhanced postprandial glucagonlike peptide-1 (GLP-1) secretion being cited as the most important (3, 8, 24). However, the primary role of GLP-1 as a mediator of the beneficial effect of RYGB on glycemic control is debated (25, 26). It has also been reported that release of glucose, via intestinal gluconeogenesis, into the portal vein of mice that underwent enterogastric anastomosis (EGA), resulted in improved insulin sensitivity of hepatic glucose production; thus, it has been hypothesized that intestinal gluconeogenesis could account for the improvement in glucose homeostasis after RYGB (27). It should be noted that EGA is not similar to RYGB, because the Roux-en-Y configuration is not constructed and no intestinal segment is representative of the Roux limb. Also, two recent reports in obese diabetic animals and in humans with type 2 diabetes and our study did not find evidence for induction of intestinal gluconeogenesis after RYGB (28, 29). A decrease in intestinal glucose absorptive capacity due to the exclusion of the duodenum after RYGB has also been

proposed as a mechanism underlying the improvement in glycemic control (11), but other studies have found that RYGB does not suppress glucose absorption from the intestinal lumen (10, 30-32). Our study shows that changes in the metabolism of the Roux limb itself may play a direct role in the improvement in glucose homeostasis after RYGB. We report that the Roux limb exhibits reprogramming of intestinal glucose metabolism to meet the increased bioenergetic demands of intestinal remodeling. We show that intestinal remodeling and reprogramming of intestinal glucose metabolism are triggered by the exposure of the Roux limb to undigested nutrients. We demonstrate that reprogramming of intestinal glucose metabolism renders the intestine amajor organ for glucose disposal, contributing to the improvement in glycemic control afterRYGB. Enhancing intestinal glucose uptake and utilization could offer an opportunity to regulate wholebody glucose disposal and improve glycemic control in type 2 diabetes. Exploitation of the changes that occur in intestinal metabolism after RYGB could represent an approach to bypass the bypass, that is, to replace the gastric bypass by equally effective, but less invasive, treatments for obesity-related diabetes.

Supplementary Material

Refer to Web version on PubMed Central for supplementary material.

Acknowledgments

We thank N. Li for help with tissue sectioning, G. Gorski for help with electron microscopy, M. Markle and M. Luitje for help with biodistribution analysis, and A. Moses for help with lipid analysis. This research was supported by funds from the Department of Medicine and the Clinical and Translational Executive Committee at Boston Children's Hospital (N. Stylopoulos) and grants T32DK007191 (N.K.G.) and F32DK095558 (N. Saeidi) from the National Institutes of Health (NIH). We used the core services of the Lipidomics Lab at the Nutrition Obesity Research Center of the University of Michigan (Ann Arbor, MI), which is supported by grant DK089503 from NIH.

References

1. Buchwald H, et al. JAMA. 2004; 292:1724–1737. [PubMed: 15479938]
2. Sjöström L, et al. Swedish Obese Subjects Study Scientific Group, N Engl J Med. 2004; 351:2683–2693.
3. Stefater MA, Wilson-Pérez HE, Chambers AP, Sandoval DA, Seeley RJ. Endocr Rev. 2012; 33:595–622. [PubMed: 22550271]
4. Mingrone G, et al. N Engl J Med. 2012; 366:1577–1585. [PubMed: 22449317]
5. Schauer PR, et al. N Engl J Med. 2012; 366:1567–1576. [PubMed: 22449319]
6. Carlsson LM, et al. N Engl J Med. 2012; 367:695–704. [PubMed: 22913680]
7. Pories WJ, et al. Ann Surg. 1995; 222:339–352. [PubMed: 7677463]
8. Laferrère B. Endocrine. 2011; 40:162–167. [PubMed: 21853297]
9. Cummings DE. Nat Med. 2012; 18:656–658. [PubMed: 22561818]
10. Bradley D, et al. J Clin Invest. 2012; 122:4667–4674. [PubMed: 23187122]
11. Stearns AT, Balakrishnan A, Tavakkolizadeh A. Am J Physiol Gastrointest Liver Physiol. 2009; 297:G950–G957. [PubMed: 20501442]
12. Mumphrey MB, Patterson LM, Zheng H, Berthoud HR. Neurogastroenterol Motil. 2013; 25:e70–e79. [PubMed: 23095091]
13. Spak E, et al. Histopathology. 2010; 57:680–688. [PubMed: 21054493]
14. Taqi E, et al. J Pediatr Surg. 2010; 45:987–995. [PubMed: 20438940]

15. le Roux CW, et al. Ann Surg. 2010; 252:50–56. [PubMed: 20562614]
16. Bueter M, et al. Gastroenterology. 2010; 138:1845–1853. 1853.e1. [PubMed: 19931268]
17. Kucharczyk J, Nestoridi E, Kvas S, Andrews R, Stylopoulos N. J Surg Res. 2013; 179:e91–e98. [PubMed: 22504136]
18. Nestoridi E, Kvas S, Kucharczyk J, Stylopoulos N. Endocrinology. 2012; 153:2234–2244. [PubMed: 22416083]
19. Materials and methods are available as supplementary materials on Science Online.
20. Lunt SY, Vander Heiden MG. Annu Rev Cell Dev Biol. 2011; 27:441–464. [PubMed: 21985671]
21. Vander Heiden MG, Cantley LC, Thompson CB. Science. 2009; 324:1029–1033. [PubMed: 19460998]
22. Thorens B. Am J Physiol. 1996; 270:G541–G553. [PubMed: 8928783]
23. Pácha J. Physiol Rev. 2000; 80:1633–1667. [PubMed: 11015621]
24. Falkén Y, Hellström PM, Holst JJ, Näslund E. J Clin Endocrinol Metab. 2011; 96:2227–2235. [PubMed: 21543426]
25. Isbell JM, et al. Diabetes Care. 2010; 33:1438–1442. [PubMed: 20368410]
26. Wilson-Pérez HE, et al. Diabetes. 2013; 62:2380–2385. [PubMed: 23434938]
27. Troy S, et al. Cell Metab. 2008; 8:201–211. [PubMed: 18762021]
28. Wolff BS, Meirelles K, Meng Q, Pan M, Cooney RN. Am J Physiol Gastrointest Liver Physiol. 2009; 297:G594–G601. [PubMed: 19556357]
29. Hayes MT, Foo J, Besic V, Tychinskaya Y, Stubbs RS. Obes Surg. 2011; 21:759–762. [PubMed: 21547404]
30. Rubino F, et al. Ann Surg. 2006; 244:741–749. [PubMed: 17060767]
31. Rodieux F, Giusti V, D'Alessio DA, Suter M, Tappy L. Obesity (Silver Spring). 2008; 16:298–305. [PubMed: 18239636]
32. Wang G, et al. Obes Surg. 2012; 22:1263–1267. [PubMed: 22527599]

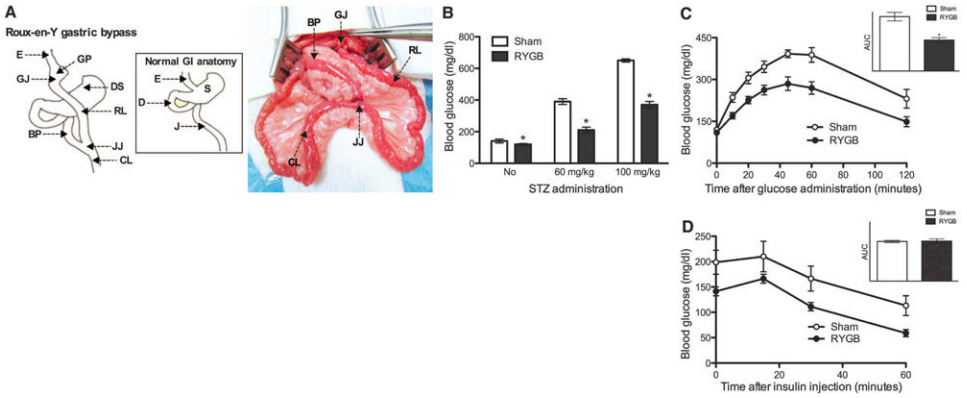

Fig. 1. RYGB improves glycemic control

(A) Schematic drawing of RYGB (left). Intraoperative picture of RYGB in rats (right). RYGB in rats closely resembles the procedure performed in humans. The stomach (S) is divided, and a small gastric pouch is created (GP). The jejunum (J) is transected, and the distal part is brought up and connected through a gastro-jejunostomy (GJ) to the GP [this jejunal loop is called the Roux limb (RL)]. The continuation of the gastrointestinal (GI) tract is reestablished by reconnecting at the jejuno-jejunostomy (JJ), the proximal part of the jejunum further down to the RL [this is called the biliopancreatic limb (BP) because it drains the gastric, hepatic, and pancreatic secretions]. The part of the small intestine distal to the JJ is called the common limb (CL). RYGB reconfigures the GI tract and alters the flow of nutrients; nutrients flow from the esophagus (E) to the GP and then to the RL directly, bypassing the distal stomach (DS), the duodenum (D), and part of the proximal jejunum. Thus, the RL is exposed to undigested nutrients; the BP is exposed to the gastric, hepatic, and pancreatic secretions but no nutrients; and the CL is exposed to a mixture of nutrients with the gastric, hepatic, and pancreatic secretions. (B) Blood glucose levels were lower in RYGB-treated rats in comparison with sham-operated rats, 7 days after diabetes was induced by the administration of STZ. (C) RYGB-treated GK rats exhibited better glucose excursion curves after oral glucose administration. The inset shows the area under the curve (AUC) of the oral glucose tolerance test. (D) There was no difference in the insulin tolerance test between RYGB-treated and sham-operated GK rats. The inset shows the AUC of the insulin tolerance test. [(B) to (D)] N = 5 to 7 rats, 2 months postoperatively; mean T SEM; *P < 0.05; unpaired t test.

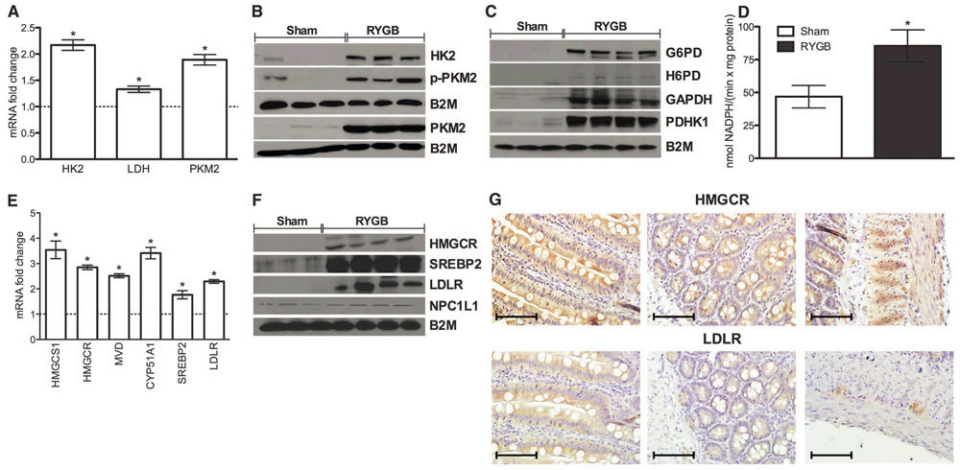

Fig. 2. RYGB increases the gene and protein expression levels of key factors and enzymes involved in glucose and cholesterol metabolism in the Roux limb

(A to C) RNA and protein levels of glycolytic enzymes and G6PD were increased in the Roux limb of RYGB-treated rats. B2M, b2 microglobulin. (D) The enzymatic activity of G6PD was increased in the Roux limb of RYGB-treated rats. (E and F) RNA and protein levels of factors and enzymes involved in cholesterol biosynthesis and uptake were increased in the Roux limb of RYGB-treated rats. HMGCS1, 3-hydroxy-3-methylglutaryl-CoA synthase 1; HMGCR, 3-hydroxy-3-methylglutaryl-CoA reductase; MVD, mevalonate (diphospho) decarboxylase; CYP51A1, cytochrome P450, family 51, subfamily A, polypeptide 1 (lanosterol 14-a demethylase); SREBP2, sterol regulatory element binding protein 2; LDLR, low-density lipoprotein receptor. There was no difference in the protein levels of Niemann-Pick C1-like 1 (NPC1L1). (G) Representative images of Roux limb sections of RYGB-treated rats stained with antibodies against HMGCR and LDLR (scale bar, 100 mm). Left to right: villi, crypts, and muscular layer. HMGCR expression was increased in the villi, the crypt cells, and the muscular layer while LDLR expression was increased in the villi and in the ganglia of the muscular layer. [(A) to (G)] N = 7 to 9 rats; [(A) to (F)] 2 months postoperatively; the results were reproduced at 1 and 6 months postoperatively; (G) 2 months postoperatively; mean T SEM; *$P < 0.05$; [(A) and (E)] one sample t test; (D) unpaired t test.

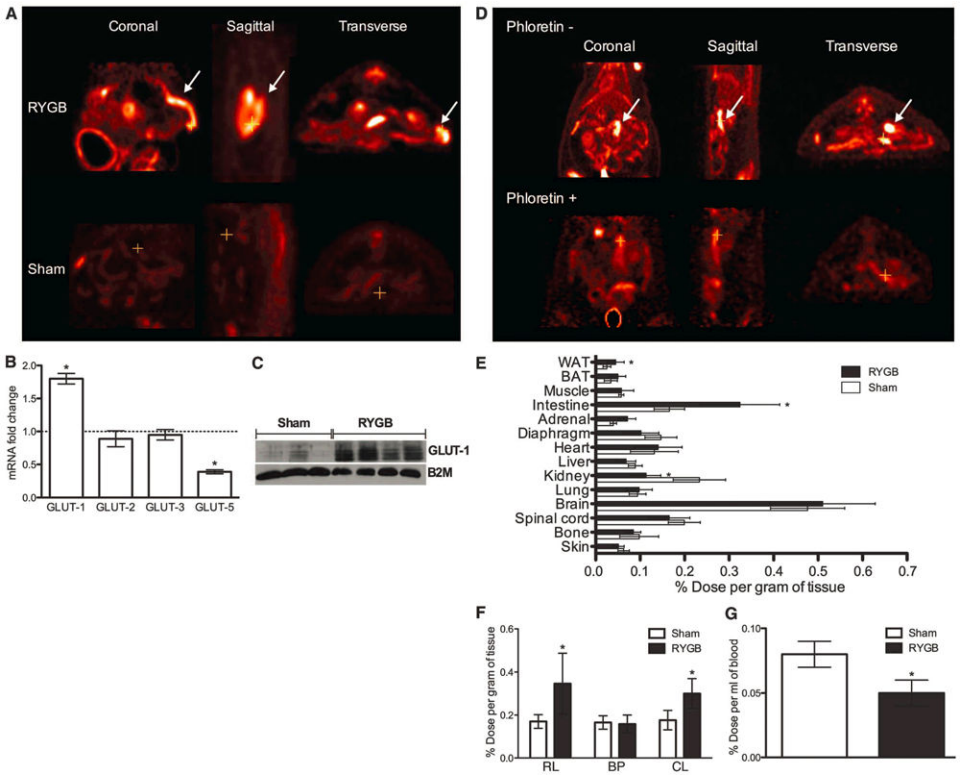

Fig. 3. RYGB enhances intestinal GLUT-1 mediated basolateral glucose uptake and utilization, which contributes to the improved whole-body glucose disposal

(A) Representative images of whole-body [18F]FDG PET/CT scanning in RYGB-treated and sham-operated rats. [18F]FDG uptake is colorcoded, and areas of increased signal exhibit red-orange color. There was intense [18F]FDG uptake by the Roux limb (marked with an arrow) of RYGB-treated rats in comparison with the corresponding jejunum of sham-operated rats. The cross indicates the exact same point of the intestine in all images. (B and C) GLUT-1 RNA and protein levels were increased in the Roux limb of RYGB-treated rats. (D) Representative images of whole-body [18F]FDG PET/CT scanning in RYGBtreated rats, with or without the administration of phloretin, a GLUT-1 inhibitor. Phloretin substantially blunted [18F]FDG uptake by the Roux limb (marked with an arrow). The cross indicates the exact same point of the intestine in all images. (E and F) [18F]FDG biodistribution analysis in RYGB-treated and shamoperated rats demonstrated higher [18F]FDG uptake by the intestine of RYGB-treated rats. WAT, white adipose tissue; BAT, brown adipose tissue. The RL of RYGBtreated rats displayed the highest [18F]FDG uptake. The uptake by the CL of RYGB-treated rats was also increased. There was no difference in the [18F]FDG uptake between the BP of RYGB-treated rats and the corresponding intestinal segment of sham-operated rats. The [18F]FDG uptake was constant along the intestine of sham-operated rats. (G) Consistent with improved whole-body glucose disposal, RYGB-treated rats exhibited lower [18F]FDG signal in the blood. [(A) to (G)] N = 7 to 9 rats; [(A) to (C)] and [(E) to (G)] 2 months postoperatively; the results were reproduced at 1 and 6 months postoperatively; (D) 6 months postoperatively; mean T SEM; *P < 0.05; (B) one sample t test; [(E) to (G)] unpaired t test.

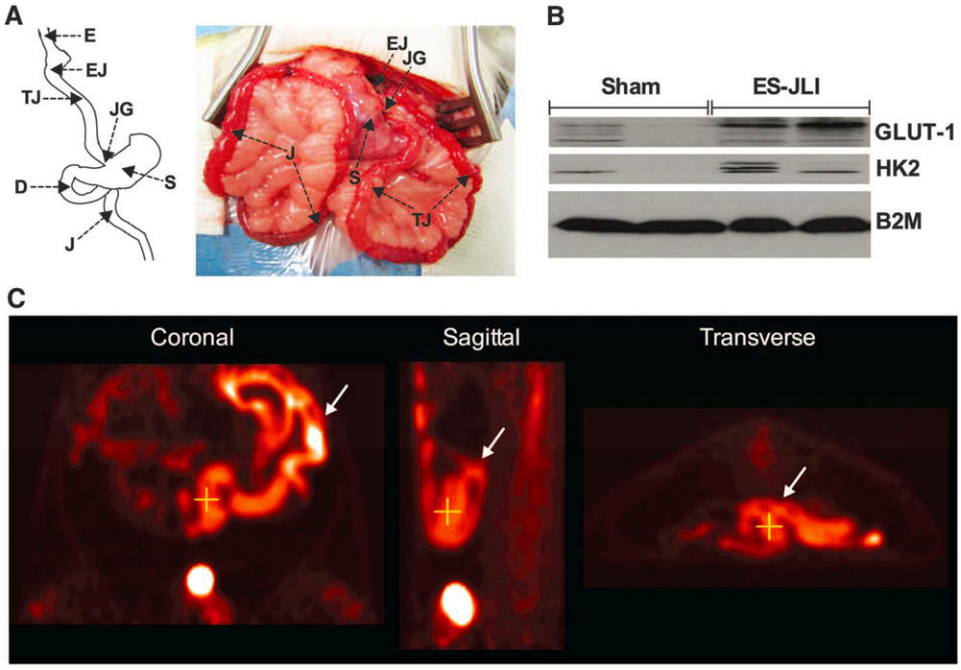

Fig. 4. Reprogramming of intestinal glucosemetabolism is triggered by the exposure of the Roux limb to undigested nutrients

(A) Schematic drawing (left) and intraoperative picture (right) of the ES-JLI rat model. A loop of jejunum is transected and transposed between the esophagus and the stomach without performing any other anatomic alterations of the RYGB procedure; that is, the stomach is not divided, the duodenum is not excluded, and the continuity of the gastrointestinal tract remains intact. Nutrients flow from the esophagus (E) through the esophago-jejunostomy (EJ) to the transposed jejunal loop (TJ) and then through the jejuno-gastrostomy (JG) to the stomach (S), the duodenum (D), the jejunum (J), and the rest of the gastrointestinal tract. (B) GLUT-1 and HK2 protein levels were increased in the transposed jejunal loop of ES-JLI–treated rats. (C) Representative images of whole-body [18F]FDG PET/CT scanning in ES-JLI–treated rats. [18F]FDG uptake is color-coded, and areas of increased signal exhibit red-orange color. There was intense [18F]FDG uptake by the transposed jejunal loop (marked with an arrow) of ES-JLI–treated rats. The cross indicates the exact same point of the intestine in all images. [(B) and (C)] N = 5 to 7 rats, 1 month postoperatively; the results were reproduced at 6 months postoperatively.